Developmental Cell
Article

Phospho-Regulated Interaction between Kinesin-6 Klp9p and Microtubule Bundler Ase1p Promotes Spindle Elongation

Chuanhai Fu,[1] Jonathan J. Ward,[2] Isabelle Loiodice,[1,3] Guilhem Velve-Casquillas,[1,3] Francois J. Nedelec,[2,*] and Phong T. Tran[1,3,*]
[1]Department of Cell and Developmental Biology, University of Pennsylvania, Philadelphia, PA 10104, USA
[2]Cell Biology and Biophysics Program, EMBL, Heidelberg 69117, Germany
[3]Institut Curie, CNRS UMR144, Paris 75005, France
*Correspondence: nedelec@embl.de (F.J.N.), tranp@mail.med.upenn.edu (P.T.T.)
DOI 10.1016/j.devcel.2009.06.012

SUMMARY

The spindle midzone—composed of antiparallel microtubules, microtubule-associated proteins (MAPs), and motors—is the structure responsible for microtubule organization and sliding during anaphase B. In general, MAPs and motors stabilize the midzone and motors produce sliding. We show that fission yeast kinesin-6 motor klp9p binds to the microtubule antiparallel bundler ase1p at the midzone at anaphase B onset. This interaction depends upon the phosphorylation states of klp9p and ase1p. The cyclin-dependent kinase cdc2p phosphorylates and its antagonist phosphatase clp1p dephosphorylates klp9p and ase1p to control the position and timing of klp9p-ase1p interaction. Failure of klp9p-ase1p binding leads to decreased spindle elongation velocity. The ase1p-mediated recruitment of klp9p to the midzone accelerates pole separation, as suggested by computer simulation. Our findings indicate that a phosphorylation switch controls the spatial-temporal interactions of motors and MAPs for proper anaphase B, and suggest a mechanism whereby a specific motor-MAP conformation enables efficient microtubule sliding.

INTRODUCTION

Mitosis occurs in distinct phases defined by changes in chromosome and spindle dynamics. In general, bipolar spindle formation occurs in prophase. Chromosome capture and alignment occur in metaphase. Chromosome segregation occurs in anaphase. Telophase marks spindle breakdown and the start of cytokinesis. Anaphase is further categorized as anaphase A, where the chromosomes are segregated to the spindle poles, and anaphase B, where the spindle can undergo dramatic elongation to ensure that the segregated chromosomes are further separated. While mechanisms of chromosome segregation during anaphase A have been the focus of intense studies (Cheeseman and Desai, 2008; Tanaka and Desai, 2008), mechanisms regulating spindle elongation during anaphase B are less well understood, and may require complex interplay between regulatory proteins, motors, and MAPs.

Anaphase B requires a proper bipolar spindle containing the midzone, a region of interdigitating microtubule overlap halfway between the spindle poles. In eukaryotes, the conserved microtubule-associated protein Ase1/PRC1, the mitotic kinesin-5 motor, and dynein play important roles in the formation of the spindle midzone and subsequent force production for spindle elongation (Maiato et al., 2004; Mogilner et al., 2006; Scholey et al., 2003; Sharp et al., 2000). Ase1/PRC1 bundles antiparallel microtubules at the midzone and gives structural integrity to the spindle. Cells lacking functional Ase1/PRC1 exhibit disorganized midzone microtubules and subsequent collapsed or broken spindles during metaphase and anaphase (Loiodice et al., 2005; Mollinari et al., 2002; Schuyler et al., 2003; Verni et al., 2004; Yamashita et al., 2005). Kinesin-5 (e.g., human Eg5) localizes at the poles and the midzone. Cells lacking functional kinesin-5 form monopolar spindles early in mitosis (Hagan and Yanagida, 1990, 1992; Hoyt et al., 1992; Kapoor et al., 2000; Roof et al., 1992). During anaphase B, kinesin-5 can produce force to slide midzone microtubules outward, thus producing spindle elongation (Kapitein et al., 2005; Straight et al., 1998). Interestingly, dynein plays a role during anaphase B without the need to localize at the spindle midzone. Dynein localizes to the cell cortex and interacts with the spindle pole-nucleated astral microtubules to produce pulling forces, which lengthen the spindle during anaphase B (Carminati and Stearns, 1997; Fink et al., 2006; Nguyen-Ngoc et al., 2007; O'Connell and Wang, 2000; Schmidt et al., 2005).

Other mitotic motors located at the spindle midzone include kinesin-4 (e.g., human KIF14) and kinesin-6 (e.g., human CHO1 and MKLP1). Surprisingly, they have not been implicated in spindle elongation during anaphase B. Instead, they appear to play a signaling role at telophase, regulating subsequent cytokinesis. Cells lacking functional kinesin-4 or kinesin-6 failed to complete cytokinesis (Gruneberg et al., 2006; Kuriyama et al., 2002; Matuliene and Kuriyama, 2002; Mishima et al., 2002).

Motors and MAPs act in concert throughout mitosis. Their interactions are often regulated by kinases and phosphatases in a cell-cycle-dependent manner. It appears that Ase1/PRC1 is phosphorylated by the cyclin-dependent kinase Cdk1 and dephosphorylated Cdk1-antagonist phosphatase Cdc14.

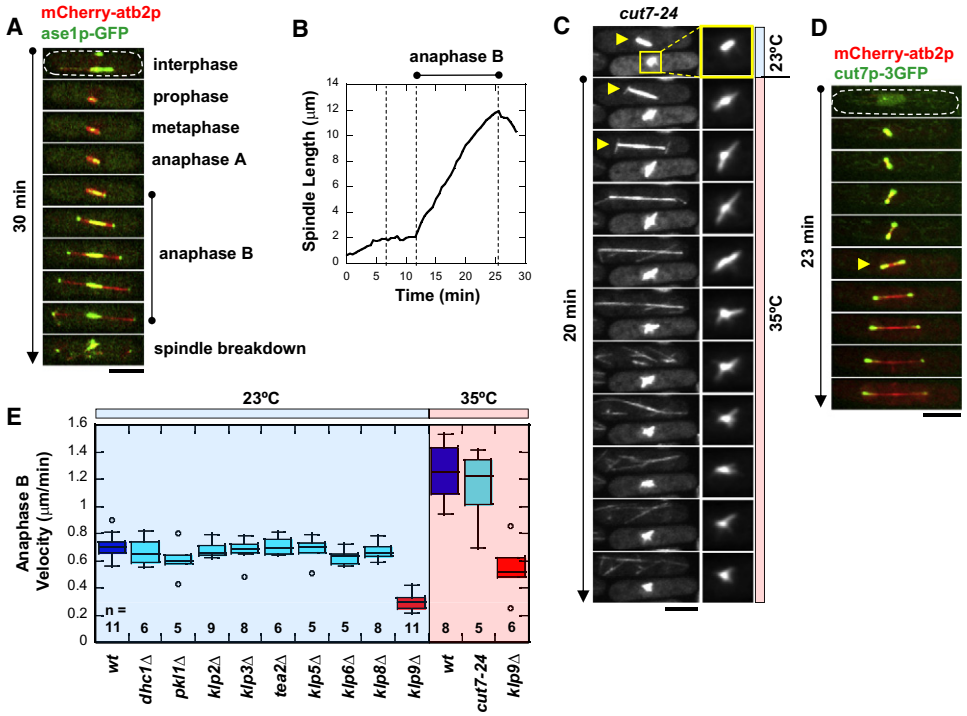

Figure 1. Fission Yeast Kinesin-6 Klp9p Is Involved in Anaphase B Spindle Elongation

(A) Time-lapse images of cell expressing mCherry-atb2p (tubulin) and ase1p-GFP through different phases of mitosis. Ase1p stabilizes the spindle midzone throughout anaphase B (Loiodice et al., 2005; Yamashita et al., 2005). Bar, 5 μm.

(B) Typical wild-type spindle length versus time plot. Anaphase B is marked by a dramatic increase in spindle length and spindle elongation velocity.

(C) Temperature shift experiment of *cut7-24* mutant cells expressing GFP-atb2p. Within 2 min of shifting to the restrictive temperature of 35°C, the metaphase cell (bottom cell) immediately exhibited spindle collapse, which became a monopolar spindle (see enlargement box) (Hagan and Yanagida, 1990, 1992). In contrast, the anaphase cell (top cell) continued through anaphase B spindle elongation (yellow arrow). Bar, 5 μm.

(D) Time-lapse images of cell expressing mCherry-atb2p (tubulin) and cut7p-3GFP. No cut7p-3GFP was observed at the anaphase B spindle midzone. Bar, 5 μm.

(E) Box plot comparison of anaphase B spindle elongation velocities in wild-type cells and motor mutant cells. Only *klp9Δ* shows a significant decrease in velocity. At the higher temperature required for *cut7-24*, spindle elongation velocity increased for both wild-type and *klp9Δ* correspondingly.

Phospho-regulation allows Ase1/PRC1 to act as a major scaffolding protein at the midzone to recruit motors, MAPs, and other regulatory proteins (Gruneberg et al., 2006; Jiang et al., 1998; Khmelinskii et al., 2007; Kurasawa et al., 2004; Zhu and Jiang, 2005; Zhu et al., 2006). Current reports on phospho-regulation of Ase1/PRC1 at the spindle midzone dealt primarily with its subsequent role as a scaffold for other proteins involved in cytokinesis, and not with its role in spindle elongation (Jiang et al., 1998; Khmelinskii et al., 2007; Zhu and Jiang, 2005).

The fission yeast *Schizosaccaromyces pombe* is a good model to study mechanisms of anaphase B. It has distinct phases of mitosis, which resemble those of mammalian cells, and in particular, a prominent anaphase B characterized by dramatic spindle elongation (Mallavarapu et al., 1999; Nabeshima et al., 1998; Sagolla et al., 2003). Importantly, fission yeast lacks the dynein-dependent astral microtubule pulling forces and kinesin-dependent microtubule flux at the spindle poles that are present in higher eukaryotes (Khodjakov et al., 2004; Tolic-Norrelykke et al., 2004), making its spindle midzone the sole structure responsible for anaphase B, and thus relatively simple for molecular dissection.

We describe here a function of the fission yeast kinesin-6 klp9p. Using a combination of biochemistry and live-cell imaging analyses, we show that prior to anaphase B, cdc2p (homolog of Cdk1) phosphorylates klp9p and the microtubule bundler ase1p, which maintains their spatial separation. At the onset of anaphase B, clp1p (also known as flp1p [Cueille et al., 2001], homolog of Cdc14) dephosphorylates klp9p and ase1p, allowing them to physically bind to each other at the spindle midzone to initiate spindle elongation. Deletion of klp9p and/or the motor-dead version of klp9p attenuate spindle elongation velocity. Phosphomimic versions of klp9p and ase1p and/or the inactive version of the phosphatase clp1p also attenuate spindle elongation velocity. FRAP analyses show that klp9p and ase1p are more mobile when not interacting with each other. Using computer simulation we predict that optimal spindle elongation may only be achieved when flexible klp9p binds to and adopts the antiparallel configuration of ase1p. Our results define a molecular pathway linking motors and MAPs, and cell-cycle-dependent regulatory kinases and phosphatases.

RESULTS

Fission yeast has distinct phases during mitosis (Figure 1A) (Mallavarapu et al., 1999; Nabeshima et al., 1998; Sagolla et al.,

2003). In particular, anaphase B shows a well-defined increase in spindle length and spindle elongation velocity (Figure 1B). We reasoned that anaphase B is likely to require molecular motors located along the spindle midzone to produce sliding forces. We therefore examined the localization of motors to the midzone by imaging GFP-tagged versions, and tested all motors for defects in spindle elongation by imaging each individual motor deletion or mutant.

The fission yeast genome has nine kinesins (*pkl1*$^+$, *klp2*$^+$, *klp3*$^+$, *tea2*$^+$, *klp5*$^+$, *klp6*$^+$, *cut7*$^+$, *klp8*$^+$, and an uncharacterized SPBC2D10.21c) and one dynein (*dhc1*$^+$). Sequence analysis revealed that the uncharacterized kinesin belongs to the kinesin-6 family. We named it *klp9*$^+$. Deletion of *klp9*$^+$ produced viable cells (see below). Individual deletion of all other motors have been reported to also produce viable cells, except for *cut7*$^+$ (Brazer et al., 2000; Browning et al., 2000; Garcia et al., 2002a, 2002b; Hagan and Yanagida, 1990, 1992; Hiraoka et al., 2000; Pidoux et al., 1996; Troxell et al., 2001; West et al., 2002, 2001). We therefore compared anaphase B velocities of wild-type and all motor deletion strains. Strains *dhc1Δ*, *pklΔ*, *klp2Δ*, *klp3Δ*, *tea2Δ*, *klp5Δ*, and *klp6Δ* all showed similar spindle elongation velocities during anaphase B compared to wild-type (Figure 1E). (Parameters of spindle dynamics throughout this study are summarized in Tables S3, S4, and S5 available online.)

Deletion of kinesin-5 *cut7*$^+$ was not viable, so we tested the nonfunctional temperature-sensitive mutant *cut7-24* (Hagan and Yanagida, 1990, 1992). We constructed a microfluidic temperature-control device (unpublished data), which allows a rapid (10 s) and robust temperature shift between 23°C and 35°C while cells are being imaged on the microscope. *Cut7-24* cells were first imaged at the permissive 23°C, where cells were in various stages of the cell cycle. We then shifted and maintained cells at the nonpermissive 35°C. Interphase cells subsequently became blocked in mitosis, exhibiting monopolar spindles, consistent with previous reports (Hagan and Yanagida, 1990, 1992). In some instances, we were able to observe two adjacent cells going through mitosis (Figure 1C). The metaphase cell, when shifted to 35°C, exhibited spindle collapse and became a monopolar spindle within 2 min after the temperature shift (Figure 1C). The monopolar spindle was a terminal phenotype. This suggested that the *cut7-24* mutant responds within 2 min of the temperature shift and is a relatively fast-acting mutant. Interestingly, the adjacent anaphase cell continued through anaphase B (Figure 1C) at a similar anaphase B velocity as wild-type cells at the same 35°C temperature (Figure 1E). This indicated that *cut7*$^+$ is important for spindle formation and the structural integrity of the metaphase spindle (Hagan and Yanagida, 1990, 1992), but may not be important for anaphase B spindle elongation. Consistent with its lack of effect on anaphase B velocity, we failed to observe cut7p-3GFP at the spindle midzone during anaphase B (Figure 1D).

Our analyses of all motors revealed that only *klp9Δ* showed a significant decrease in anaphase B velocity at both temperature ranges (Figure 1E). We note that there may be other unidentified mechanisms responsible for microtubule sliding during anaphase B that contribute to the total anaphase B velocity, such as different motors acting in concert. Nevertheless, *klp9*$^+$ alone suffices to account for the majority of anaphase B velocity. We next focused on the function of *klp9*$^+$.

Klp9p Is a Kinesin-6 Involved in Anaphase B Spindle Elongation

First, we examined the dynamics of klp9p throughout the cell cycle in conjunction with microtubules. From interphase to the onset of anaphase B, klp9p-GFP localized isotropically in the nucleoplasm (Figure 2A). At the onset of anaphase B, klp9p bound dramatically to the spindle and appeared to focus at the spindle midzone, the site of antiparallel overlapping microtubules (Figure 2A). At the end of anaphase B, klp9p localized briefly to the so-called postanaphase arrays (PAA) of microtubules (Hagan, 1998) before returning to the nucleoplasm (Figure 2A). Klp9p localization to the spindle midzone and PAA microtubules appeared consistent with previously reported roles for the kinesin-6 family in regulating the exit from mitosis and the entry into cytokinesis (Guse et al., 2005; Kuriyama et al., 2002; Matuliene and Kuriyama, 2002; Mishima et al., 2004). However, kymographs showing that klp9p localization at the spindle midzone coincides with the onset of anaphase B (Figure 2B), and the result that *klp9Δ* cells showed decreased anaphase B spindle elongation velocity (Figure 1E), prompted us to investigate its role in spindle elongation.

In vitro binding assays of recombinant klp9p revealed that it can exist in dimeric and tetrameric forms (Figure 2C), thus implying that it can crosslink and slide microtubules apart, similar to the kinesin-5 Eg5 (Kapitein et al., 2005). Therefore, we examined the deletion and the motor-dead (md) versions of klp9p. The motor-dead *klp9*^{md} has a mutated ATP-hydrolysis domain rendering the motor head inactive (Matuliene and Kuriyama, 2002). Wild-type, *klp9Δ*, *klp9Δ* cells expressing *klp9*^{md}, and *klp9Δ* cells expressing *klp9*^{wt} were assayed for anaphase B spindle elongation (Figure 2D). Wild-type and *klp9Δ* cells expressing *klp9*^{wt} exhibited similar anaphase B velocities (mean ± SD: 0.67 ± 0.06 μm/min, n = 13, and 0.58 ± 0.04 μm/min, n = 11, respectively), indicating that *klp9*^{wt} can rescue the *klp9Δ* deletion phenotype. In contrast, *klp9Δ* cells and *klp9Δ* cells expressing *klp9*^{md} showed significantly decreased velocities (0.30 ± 0.06 μm/min, n = 11, and 0.30 ± 0.04 μm/min, n = 10, respectively). We hypothesize that the fission yeast klp9p is a kinesin-6 involved in generating microtubule-sliding forces at the spindle midzone during anaphase B. To our knowledge, this may be a novel function for the kinesin-6 family.

Klp9p Interacts Physically with Ase1p at the Spindle Midzone

We and others have previously reported that fission yeast ase1p localizes to the spindle midzone and functions to stabilize the bipolar spindle (Figure 1A) (Loiodice et al., 2005; Yamashita et al., 2005) and that ase1p can autonomously target antiparallel microtubule overlap regions in vitro (Janson et al., 2007). In contrast, PRC1 has been reported to directly bind to the kinesin-4 KIF4 in order to be targeted to the spindle midzone in mammalian cells (Kurasawa et al., 2004; Zhu and Jiang, 2005). As there appear to be no homologs of kinesin-4 in fission yeast, we examined the interdependency of klp9p and ase1p targeting to the spindle midzone. Imaging revealed that at the onset of anaphase B, ase1p always appeared at the spindle midzone a few seconds before klp9p (Figure 3A). This suggests that ase1p binds to the spindle midzone earlier and independently of klp9p. We then hypothesized that ase1p may recruit klp9p to the spindle midzone.

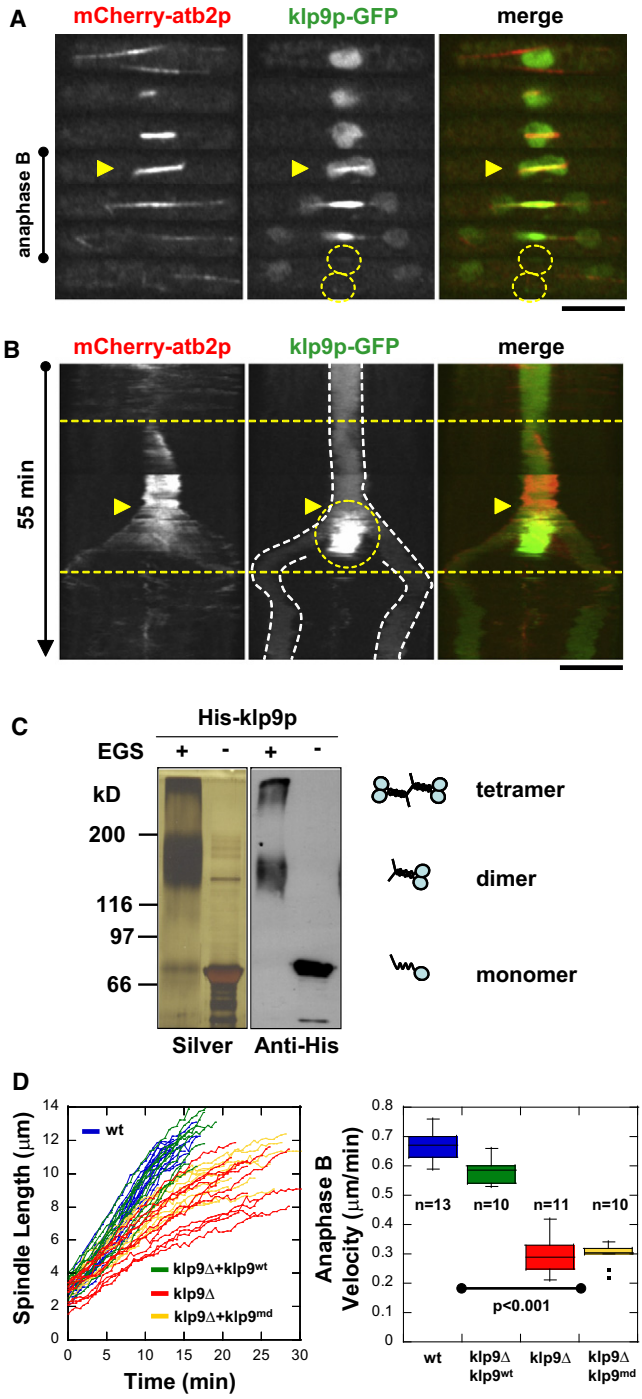

Figure 2. Klp9p May Be a Tetramer that Slides the Bipolar Spindle Apart during Anaphase B

(A) Time-lapse images of cell expressing mCherry-atb2 (tubulin) and klp9p-GFP. During interphase, prophase, metaphase, and anaphase A, klp9p-GFP is located in the nucleoplasm. At the onset of anaphase B (yellow arrow heads), klp9p-GFP goes to the spindle and the spindle midzone. At the end of anaphase B, the spindle breaks down, and klp9p-GFP is transiently at the site of the presumptive contractile ring (yellow dashed circles).

(B) Kymographs of klp9p dynamics throughout the cell cycle. Mitosis in fission yeast lasts ~30 min. Anaphase B (yellow arrow heads) marks a relatively fast spindle elongation rate of ~0.7 μm/min and lasts ~12 min before spindle breakdown. Klp9p-GFP localizes to the spindle at anaphase B onset, and focuses to the spindle midzone throughout anaphase B (yellow dashed circle). Dashed white lines mark the position of the nucleus and divided nuclei. Bar, 5 μm.

(C) EGS crosslinking of recombinant His-klp9p revealed dimers and tetramers.

(D) Comparative plot of spindle length versus time and box plot of anaphase B spindle elongation velocities of wild-type cells (WT, blue), *klp9Δ* cells expressing exogenous wild-type *klp9* (*klp9Δ+klp9*^{wt}, green), *klp9Δ* cells (*klp9Δ*, red), and *klp9Δ* cells expressing exogenous *klp9* motor dead mutant (*klp9*^{md}, yellow).

To test this hypothesis, we examined klp9p distribution in the absence of *ase1*$^{+}$. Whereas wild-type cells showed distinct and focused klp9p at the spindle midzone during anaphase B, *ase1Δ* cells showed dispersed klp9p localization throughout the spindle (Figure 3B), consistent with ase1p recruiting klp9p to the spindle midzone. Interestingly, ase1p also showed dispersed localization in *klp9Δ* cells (Figure 3C), suggesting that once bound together, klp9p can transport and focus ase1p to the spindle midzone (Zhu et al., 2005; Zhu and Jiang, 2005). To further test for physical interactions between klp9p and ase1p, we performed in vitro binding assays of recombinant klp9p and ase1p. Klp9p was observed to bind directly to ase1p (Figure 3D). Our mapping studies reveal that the domain responsible for binding klp9p lies at *ase1*$^{416-639}$ (Figure 3D). Taken together, we hypothesize that klp9p can bind autonomously to the spindle microtubules at the onset of anaphase B, but efficient targeting to the midzone requires physical binding to ase1p. Importantly, the *klp9Δ-ase1Δ* double deletion are synthetically lethal (our unpublished data), suggesting that this combination of motor and MAP is essential for anaphase B spindle elongation.

Cdc2p and Clp1p Regulate the Phosphorylation States of Klp9p and Ase1p

Budding yeast Ase1 has previously been shown to be dephosphorylated by Cdc14 at the end of mitosis (Khmelinskii et al., 2007), suggesting a role for the cyclin-dependent kinase Cdk1 and its antagonist phosphatase Cdc14 in the regulation of Ase1 during the cell cycle. To determine if the Cdk1-Cdc14 pair also regulates klp9p and ase1p in fission yeast, we examined their localization at the spindle and the effects of their activity on klp9p and ase1p. Fission yeast cdc13p (homolog of cyclin-B and binding partner of cdc2p, the homolog of Cdk1) and clp1p (homolog of Cdc14) have been shown previously to localize to the spindle at mitosis (Cueille et al., 2001; Trautmann et al., 2001, 2004; Wolfe et al., 2006). Consistent with these findings, we showed that cdc13p was associated with the spindle until the onset of anaphase B (Figure 4A). There was no visible presence of cdc13p at the midzone during anaphase B. In contrast, clp1p appeared to concentrate at the spindle midzone during anaphase B in an antagonistic manner (Figure 4A). This differential localization at the spindle during anaphase B suggested that cdc2p and clp1p may regulate the phosphorylation states of klp9p and ase1p. To test this hypothesis, we probed for phosphorylation and dephosphorylation of klp9p and ase1p by cdc2p and clp1p, respectively.

A previous phosphoproteomic mass spectrometry study in fission yeast revealed specific cdc2p-dependent phosphorylation sites on klp9p (three sites: S598, S605, and S611) and ase1p (four sites: S640, S683, S688, and S693) during mitosis

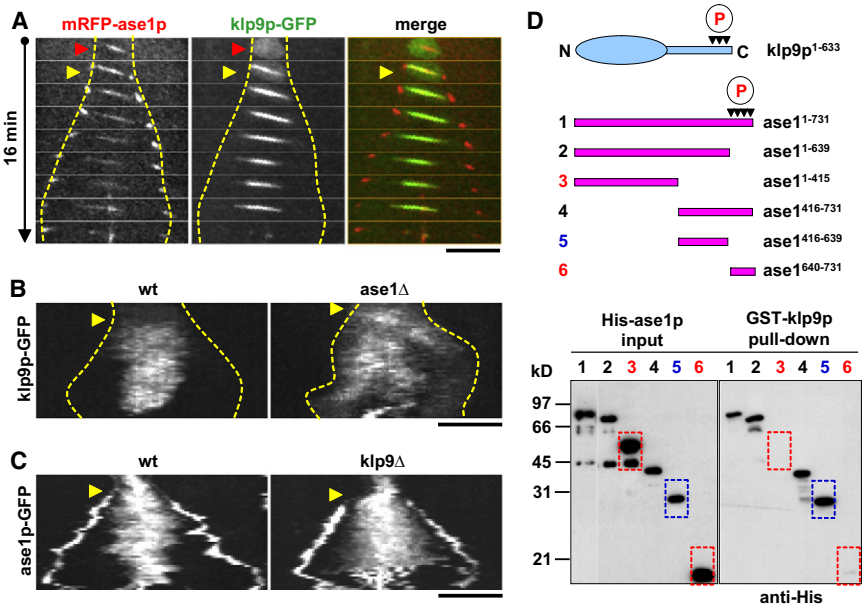

Figure 3. Klp9p Interacts with the Microtubule Bundler Ase1p In Vivo and In Vitro, and Requires Ase1p to Focus at the Spindle Midzone

(A) In vivo colocalization of klp9p and ase1p at the spindle midzone during anaphase B. Time-lapse images of a cell expressing mRFP-ase1p and klp9p-GFP. Dashed yellow lines show positions of the spindle poles. The microtubule antiparallel bundler mRFP-ase1p localizes early on to the spindle (red arrow head). Subsequently, at the onset of anaphase B (yellow arrow heads), klp9p-GFP colocalizes with mRFP-ase1p at the spindle and spindle midzone. Bar, 5 μm.

(B) Kymographs of wild-type and *ase1Δ* cells expressing klp9p-GFP (anaphase B onset, yellow arrows). The wild-type cell shows a clear focusing of klp9p-GFP at the spindle midzone as anaphase B progressed. In contrast, the *ase1Δ* cell fails to focus klp9p-GFP at the midzone region.

(C) Kymographs of wild-type and *klp9Δ* cells expressing ase1p-GFP (anaphase B onset, yellow arrows). The wild-type cell shows a clear focusing of ase1p-GFP at the spindle midzone as anaphase B progressed. In contrast, the *klp9Δ* cell fails to focus ase1p-GFP at the midzone region. Bar, 5 μm.

(D) Klp9p binds to ase1p in vitro. Pull-down assays of full-length recombinant GST-klp9p with different truncated versions of recombinant His-ase1p. Schematics of klp9p and ase1p, showing multiple cyclin-dependent kinase phosphorylation sites at their carboxyl termini (red circled P). Dashed red boxes (lanes 3 and 6) indicate no physical interaction. Dashed blue boxes (lane 5) indicate physical interaction.

(Wilson-Grady et al., 2008). We created phosphoinhibit versions of klp9p and ase1p by mutating the serine into alanine (S>A) at all the reported consensus cdc2p-dependent phosphorylation motifs (Wilson-Grady et al., 2008). We note that individual mutations yielded only minor effects. We then performed in vitro phosphorylation assays using recombinant cdc2p, clp1p, klp9p, ase1p, klp9p$^{S>A}$, and ase1p$^{S>A}$. Whereas wild-type klp9p and ase1p were highly phosphorylated by cdc2p, klp9p$^{S>A}$ and ase1p$^{S>A}$ showed a dramatic decrease in cdc2p-dependent phosphorylation (Figure 4B). Interestingly, our blot revealed residual minor phosphorylation signals in both klp9p$^{S>A}$ and ase1p$^{S>A}$, suggesting that other cdc2p-dependent phosphorylation sites may be present. We next performed dephosphorylation assays on the phosphorylated proteins. The cdc2p-phosphorylated klp9p and ase1p products showed significant, but not complete, dephosphorylation by clp1p (Figure 4C). We hypothesize that cdc2p phosphorylates both klp9p and ase1p prior to anaphase B. At anaphase B onset, cdc2p activity is inhibited by clp1p (Wolfe et al., 2006), and clp1p may dephosphorylate both klp9p and ase1p. One function of cdc2p-dependent phosphorylation is to allow ase1p to transit from the cytoplasm into the nucleus during the G_2/M transition (Figures 4D and 4E). Once ase1p enters the nucleus and binds to the spindle, a second function of phosphorylation may be to prevent the physical interactions of klp9p and ase1p at the spindle midzone until anaphase B onset, when clp1p-dependent dephosphorylation of klp9p and ase1p allows the motor and MAP to physically interact for proper spindle elongation.

Klp9p and Ase1p Interaction Requires Dephosphorylation

To test this hypothesis, we performed in vitro binding assays with recombinant wild-type (i.e., not phosphorylated) and phosphomimic klp9p and ase1p. Phosphomimic versions of klp9p and ase1p were created by mutating the serine into aspartic acid (S>D) at all the reported consensus cdc2p-dependent phosphorylation sites (Wilson-Grady et al., 2008). With the exception of the phosphomimic klp9p$^{S>D}$ and ase1p$^{S>D}$, which exhibited little or no binding, all other combinations of klp9p and ase1p phosphorylation states exhibited strong differential bindings, with klp9p^{wt} and ase1p^{wt} exhibiting the strongest affinity based on the blot signal (Figure 5A). We hypothesize that clp1p-dependent dephosphorylation of both klp9p and ase1p at the onset of anaphase B enables physical interactions of motor and MAP to occur at the spindle midzone.

We next examined the consequences of the failure of klp9p and ase1p to interact at anaphase B. We reasoned that klp9p and ase1p would not physically interact if they remained phosphorylated at anaphase B (Figure 5A). One way to achieve this would be to use the phosphomimic *klp9*$^{S>D}$ and *ase1*$^{S>D}$. A second way would be to use the phosphatase inactive mutant *clp1*^{off} (Wolfe et al., 2006), which would fail to deactivate cdc2p and fail to dephosphorylate klp9p and ase1p. We analyzed klp9p and ase1p localization and spindle dynamics in the inactive mutant *clp1*^{off} and the double phosphomimic mutant *ase1*$^{S>D}$-*klp9*$^{S>D}$. In contrast to wild-type cells (Figure 5C), both the *clp1*^{off} and *ase1*$^{S>D}$-*klp9*$^{S>D}$ strains exhibited dispersed klp9p and ase1p localization, with no clear focus at the spindle midzone throughout anaphase B (Figures 5B and 5C), which is consistent with the hypothesis that klp9p-ase1p midzone localization requires clp1p-dependent dephosphorylation of both motor and MAP.

Further, whereas wild-type cells exhibited stereotypical anaphase B velocity (0.68 ± 0.09 μm/min, n = 11), mutant *clp1*^{off} and *ase1*$^{S>D}$-*klp9*$^{S>D}$ cells showed significantly decreased spindle velocities (0.35 ± 0.05 μm/min, n = 9, and 0.48 ± 0.08 μm/min, n = 12, respectively) (Figure 5D). We noted that while spindle

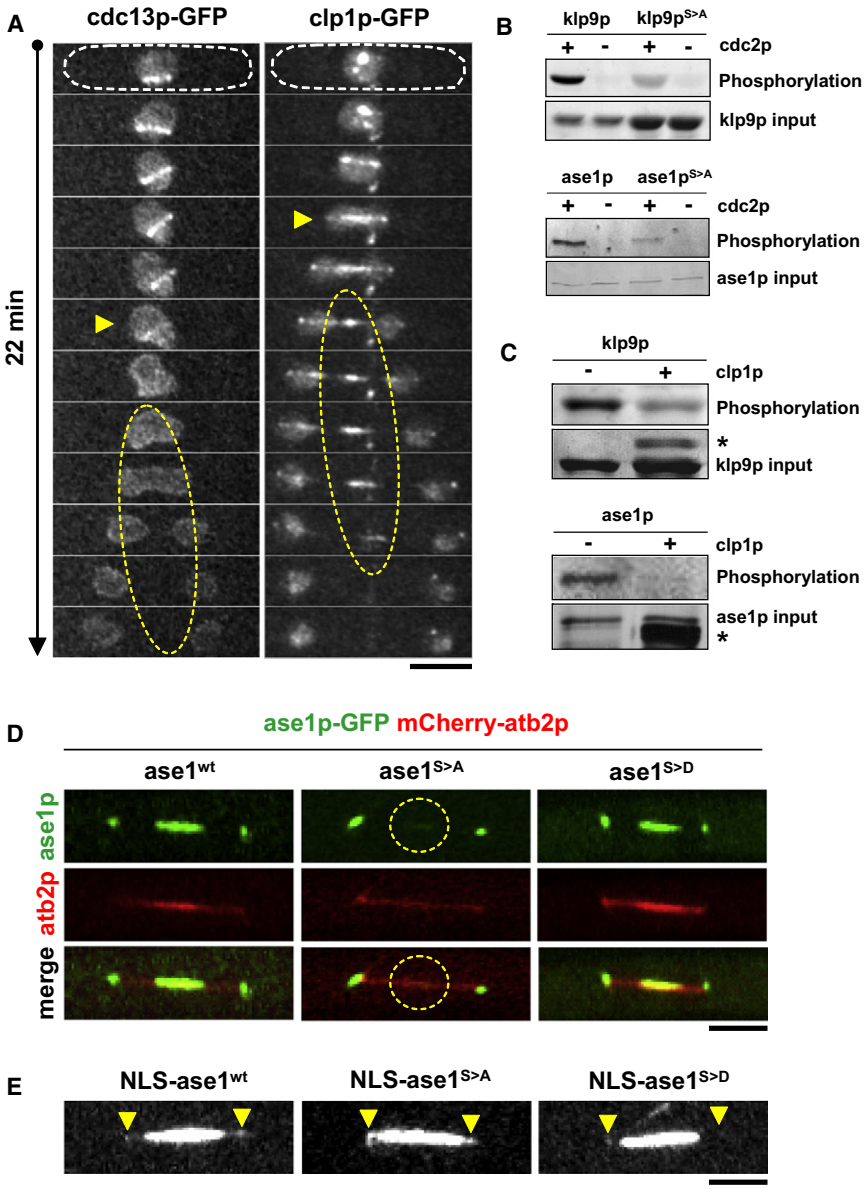

Figure 4. Kinase Cdc2p and Its Antagonist Phosphatase Clp1p Regulate the Phosphorylation States of Klp9p and Ase1p

(A) Time-lapse images of cells expressing either cdc13p-GFP (cyclin B, binding partner of cdc2p) or clp1p-GFP during mitosis. Prior to anaphase B, cdc13p-GFP localizes to the spindle. At anaphase B onset (yellow arrow head), cdc13p-GFP delocalizes from the spindle (yellow dashed oval). In contrast, prior to anaphase B, clp1p-GFP localizes to the spindle poles and kinetochores. At anaphase B onset (yellow arrow head), clp1p-GFP localizes to the spindle and subsequently the spindle midzone (yellow dashed oval). Bar, 5 μm.

(B) Klp9p and ase1p are phosphorylated by cdc2p in vitro. Recombinant His-klp9p and His-klp9p^{phosphoinhibit} (His-klp9p$^{S>A}$) and His-ase1p and His-ase1p^{phosphoinhibit} (His-ase1p$^{S>A}$) were incubated with cdc2p.

(C) Klp9p and ase1p are dephosphorylated by clp1p in vitro. Recombinant GST-klp9p and GST-ase1p were first phosphorylated by cdc2p. The products were next incubated with recombinant MBP-clp1p. Asterisks correspond to MBP-clp1p.

(D) Ase1-phosphoinhibit version ase1p$^{S>A}$ cannot enter the nucleus during closed mitosis. Shown are cells expressing mCherry-atb2 (tubulin) and GFP-tagged ase1^{wt}, ase1^{phosphoinhibit} (ase1$^{S>A}$), or ase1^{phosphomimic} (ase1$^{S>D}$). At mitosis ase1^{wt} and ase1$^{S>D}$ localize to the spindle midzone. In contrast, ase1$^{S>A}$ is not strongly visible at the spindle midzone (yellow dashed circle). Bar, 5 μm.

(E) Dual GFP- and NLS-tagged versions of ase1^{wt}, ase1^{phosphoinhibit} (ase1$^{S>A}$), or ase1^{phosphomimic} (ase1$^{S>D}$). Prominent is the strong signal of ase1^{phosphomimic} (ase1$^{S>D}$), which now can enter the nucleus. Arrowheads mark the spindle poles. Bar, 5 μm.

velocities of *ase1*$^{S>D}$-*klp9*$^{S>D}$ double mutant cells are expectedly less than those of wild-type cells, they are unexpectedly more than those of single mutant *klp9Δ* cells: compare 0.68 μm/min (WT), 0.29 μm/min (*klp9Δ*), and 0.48 μm/min (*ase1*$^{S>D}$-*klp9*$^{S>D}$) (compare Figures 2D and 5D). Indeed, *ase1*$^{S>D}$-*klp9*$^{S>D}$ velocity is half-way between wild-type and the basal *klp9Δ* velocity; i.e., the presence of klp9p, even when it does not bind to ase1p, can produce intermediate sliding velocity at ~50% attenuation between wild-type maximum velocity and basal *klp9Δ* velocity (WT > *ase1*$^{S>D}$-*klp9*$^{S>D}$ > *klp9Δ*). How can klp9p binding to ase1p produce maximum velocity? We have addressed this using computer simulation (see below).

FRAP Analyses Suggest an In Vivo Interaction between Klp9p and Ase1p

To establish a possible in vivo interaction of klp9p or ase1p, we performed FRAP experiments on cells expressing either GFP-klp9p or ase1p-GFP under the wild-type, *ase1Δ*, or *clp1*^{off} cell background (Figures 6A and 6B). We reasoned that if klp9p and ase1p are physically interacting, they would have the same mobility, and moreover, they would be less mobile as a complex than if they were separated individually. We note that due to the complexity of the experiment (e.g., the spindle is actively elongating at anaphase B, the relatively large FRAP region that covers half of the spindle midzone and thus bleaches half of the available proteins, and the processive nature of motors [Kapitein et al., 2005] and diffusive nature of MAPs [Kapitein et al., 2008a]), it may not be meaningful to extract rate constants and recovery times. We chose instead to analyze the relative percentage recovery of the different proteins. Within the 250 s of measurement, both GFP-klp9p and ase1p-GFP showed the same relatively low recovery in wild-type cells (Figure 6C), at 10% ± 6%, n = 3, and 7% ± 5%, n = 5, respectively. In contrast, in the absence of either the MAP (*ase1Δ*) or the motor (*klp9Δ*), klp9p and ase1p were more mobile (Figure 6C), with recovery of 58% ± 21%, n = 5, and 36% ± 16%, n = 4, respectively. In the *clp1*^{off} mutant, where klp9p and ase1p are expected to not

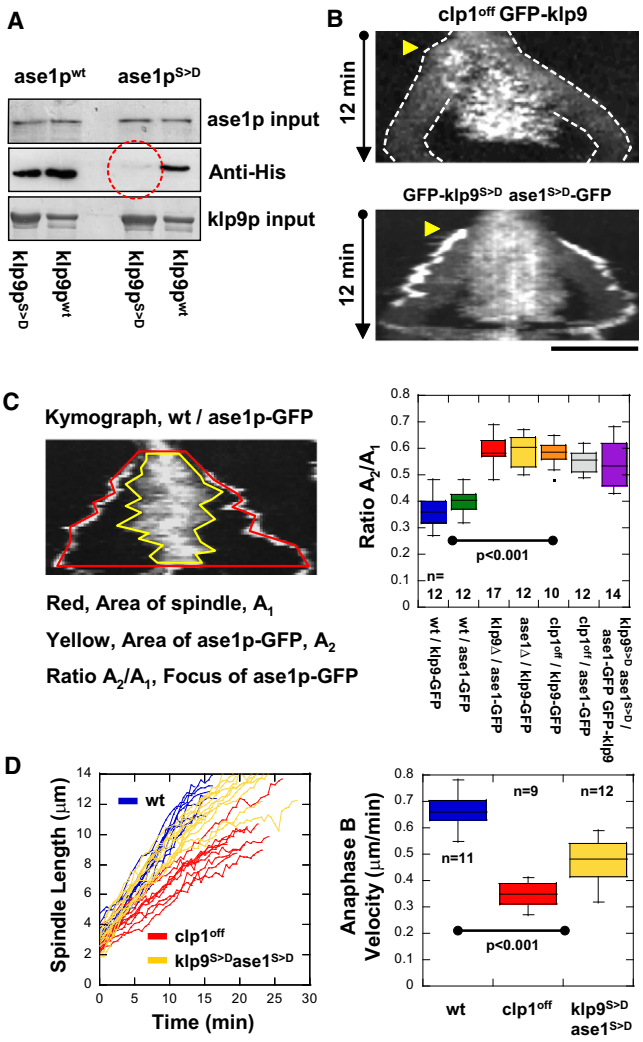

Figure 5. Dephosphorylation of Klp9p and Ase1p by the Phosphatase Clp1p Is Required for Their Efficient Binding and Proper Anaphase B Spindle Elongation

(A) Pull-down assays of recombinant GST-klp9p and GST-klp9p^{phosphomimic} (GST-klp9p$^{S>D}$) with recombinant His-ase1p and His-ase1p^{phosphomimic} (His-ase1p$^{S>D}$). The strongest binding is observed with GST-klp9p and His-ase1p. Binding is also observed with either GST-klp9p or His-ase1p phosphomimic versions. No binding is observed between GST-klp9p$^{S>D}$ and His-ase1p$^{S>D}$ (red dashed circle).

(B) Kymographs of mutant *clp1*^{off} cells and double mutant *klp9* ^{phosphomimic} *ase1*^{phosphomimic} (*klp9* $^{S>D}$*ase1*$^{S>D}$) cells expressing klp9p-GFP during mitosis. Mutant *clp1*^{off} cells, which have no phosphastase activity, and double mutant *klp9* $^{S>D}$*ase1*$^{S>D}$ cells show GFP-klp9p and ase1p-GFP dispersed to wider regions of the spindle. Bar, 5 μm.

(C) Quantification of klp9p and ase1p focusing at the spindle midzone. Kymograph of anaphase B shows two regions of interest: the area A_1 covered by the spindle (red boundary), and the area A_2 covered by klp9p-GFP or ase1p-GFP at the midzone (yellow boundary). We defined the ratio of the A_2/A_1 as the index of focusing. A box plot shows that klp9p-GFP and ase1p-GFP are highly focused at the spindle midzone in wild-type cells. In contrast, phospho mutants of *klp9* and *ase1* and *clp1*^{off} show klp9p-GFP and ase1p-GFP spread out on the spindle.

(D) Comparative plot of spindle length versus time and box plot of anaphase B spindle elongation velocity of wild-type cells (WT, blue), mutant *clp1*^{off} cells (*clp1*^{off}, red), and double mutant *klp9* ^{phosphomimic}*ase1*^{phosphomimic} cells (*klp9* $^{S>D}$*ase1*$^{S>D}$, yellow).

interact, klp9p and ase1p were also more mobile than in wild-type (Figure 6C), with recovery of 25% ± 8%, n = 3, and 61% ± 15%, n = 3, respectively. Finally, FRAP of the double phosphomimic mutant *ase1*$^{S>D}$-*klp9*$^{S>D}$ also showed motor and MAP to be more mobile than wild-type (see Figure S1). Taken together, we interpret these results as consistent with an in vivo interaction between klp9p and ase1p and with the idea that the interaction is dependent on clp1p function.

Cytosim Simulation Reveals Ase1p-Klp9p Antiparallel Binding to Microtubules

Tetrameric kinesin-5 Eg5 has been shown to be flexible and can twist as it crosslinks and moves on two microtubules in vitro (Kapitein et al., 2005). Our current work shows that klp9p is a tetrameric kinesin-6 which binds microtubules independently of its phosphorylation state, but binds to ase1p in a clp1p-dependent manner. We previously reported that ase1p may be a rigid dimer with an antiparallel configuration that binds two microtubules into a rigid antiparallel bundle (Janson et al., 2007). Therefore, we hypothesized that klp9p, like Eg5, is a flexible tetramer that can adopt both parallel and antiparallel configurations, but that binding of klp9p to antiparallel ase1p locks klp9p into an antiparallel state (Figure 7A). The parallel configuration of klp9p would not produce microtubule sliding. The antiparallel configuration of klp9p would produce maximal sliding velocity. Intermediate sliding velocities would be produced when some klp9p binds parallelly and other binds antiparallelly. We tested this hypothesis using the simulation program Cytosim (Nedelec and Foethke, 2007).

Cytosim has been used previously to model coordination between klp2p, ase1p, and microtubules in bringing about proper microtubule antiparallel organization (Janson et al., 2007). We note that the current simulation does not attempt to describe all aspects of anaphase B. It only tests the hypothesis that binding of klp9p in an antiparallel configuration would produce the maximal spindle elongation velocity. Our model assumes an initial bipolar spindle composed of five microtubules with lengths of 3 μm in each half of the spindle (Figure 7A). The overlapping midzone was set initially at 3 μm (Figure 7A). A notable feature of the anaphase B fission yeast spindle is the high concentration of ase1p and klp9p at the midzone (Figure 3), and it is possible that the effects of finite microtubule binding sites could affect spindle elongation. This property is represented in our model by imposing an 8 nm site spacing, where each site can be occupied by a single motor or MAP. The motor moves in discrete steps of 8 nm and can move only if the adjacent site is unoccupied. As the kinetic parameters of klp9p are currently unknown, we set the physical properties of klp9p to be similar to Eg5 because of their shared tetrameric structure and their related roles in anaphase B (Figure 7B) (Kapitein et al., 2008b; Kwok et al., 2006; Valentine et al., 2006a, 2006b).

The first simulation involves the spindle, described above, and 120 klp9p tetramers. This is the simplest model that results in spindle elongation and can be considered a simulation of the *ase1Δ* mutant. In this model, no ase1p molecules were present, and klp9p motility is therefore not impeded by the presence of ase1p on the microtubule lattice. Klp9p can adopt either a parallel configuration (bundling) or an antiparallel configuration (force production). This model resulted in spindles that elongate at an average rate that is similar to that observed in *ase1Δ* cells of 0.48 ± 0.15 μm/min (n = 11) (Figure 7D).

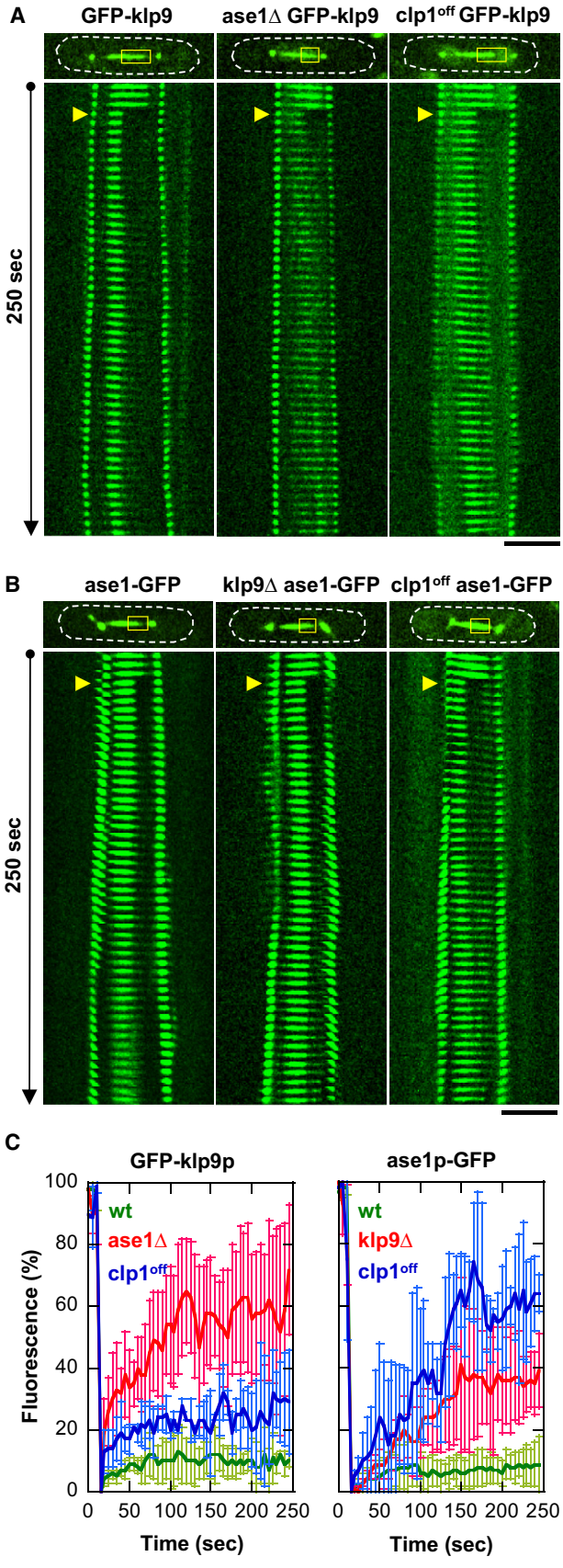

Figure 6. FRAP Analysis Suggests an In Vivo Interaction between Klp9p and Ase1p

(A) Coarse kymograph of fluorescence recovery of cells expressing GFP-klp9p under the wild-type, *ase1Δ*, or *clp1*^{off} cell background. Note that cells also express alp4p-GFP spindle pole marker to show precise spindle length and the timing of anaphase B. Yellow boxes, bleached region; yellow arrows, FRAP start. Bar, 5 μm.

(B) Coarse kymograph of fluorescence recovery of cells expressing ase1p-GFP under the wild-type, *klp9Δ*, or *clp1*^{off} cell background.

(C) Comparative plots of fluorescence recovery after bleaching. Shown are normalized fluorescent signals prebleached at 100% (mean ± SD). Left panel, GFP-klp9p in wild-type (green), *ase1Δ* (red), and *clp1*^{off} (blue). Right panel, ase1p-GFP in wild-type (green), *ase1Δ* (red), and *clp1*^{off} (blue). Note the relatively higher mobility of klp9p and ase1p in the mutant backgrounds compared to wild-type.

The second model is identical to the first, but with the addition of 100 dimers of the bundling protein ase1p. In this model, there are no direct interactions between ase1p and klp9p, and klp9p is free to adopt either a parallel or antiparallel configuration, which can be considered a simulation of the *clp1*^{off} mutant. The properties of ase1p are similar to those used to model interphase microtubule bundles (Janson et al., 2007), except that the molecule acts as a bridge with a fixed distance between the bundled microtubules. There are also two stiffness components, a component that resists microtubule sliding and a second component that resists the separation of bundled microtubules. Single-molecule studies have shown that the ase1p dimer diffuses freely on the microtubule lattice (Kapitein et al., 2008a), so the component resisting microtubule sliding is set to zero in this and other models involving ase1p. The reduced spindle elongation rate of 0.35 ± 0.05 μm/min (n = 9) observed in the *clp1*^{off} mutant is also reproduced by this model (Figures 7C and 7D). It is notable that the model maintains a constant spindle elongation velocity despite a decrease in the length of microtubule overlap at the midzone, as is also observed experimentally (compare Figures 5D and 7C). The reduced spindle elongation speed, exhibited by the model, is caused by reduced klp9p binding and impeded motility caused by the presence of ase1p dimers on the microtubule lattice. Kymographs of simulated *ase1Δ* cells also showed that klp9p is less focused at the spindle midzone compared to wild-type, in agreement with experiments (compare Figures 5C and 7E).

The final model is identical to the second, but here klp9p binds preferentially in an antiparallel configuration, which is expected to be the case in wild-type cells. We did not directly model the physical interaction between klp9p and ase1p, but instead adjusted the properties of klp9p so that it binds microtubules preferentially in an antiparallel configuration and has a slightly higher microtubule-association rate. With these adjustments the model reproduced the spindle velocity of 0.68 ± 0.09 μm/min (n = 11) observed in wild-type cells (Figure 7D). Our simple models recapitulated the experimental results and therefore showed how specific binding of klp9p to microtubules in an antiparallel orientation could increase the rate of spindle elongation, although this effect could also be explained by other mechanisms (see Discussion).

Taken together, and to our knowledge, our current work describes a novel function for the kinesin-6 klp9p in anaphase B spindle elongation and a novel mode of klp9p and ase1p interaction that is controlled by phosphorylation (Figure 7F).

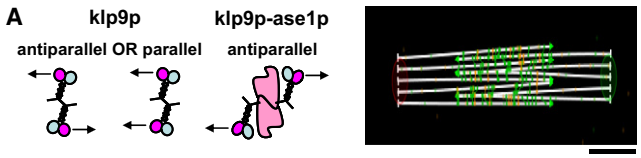

B

Property (units)	Conventional kinesin	Eg5	Simulated klp9p
Speed (nm/s)	650	16	20
Stalling force (pN)	5	9	6
Detachment rate (s^{-1})	1.6	0.025	0.5
Run length (nm)	400	N/A	40

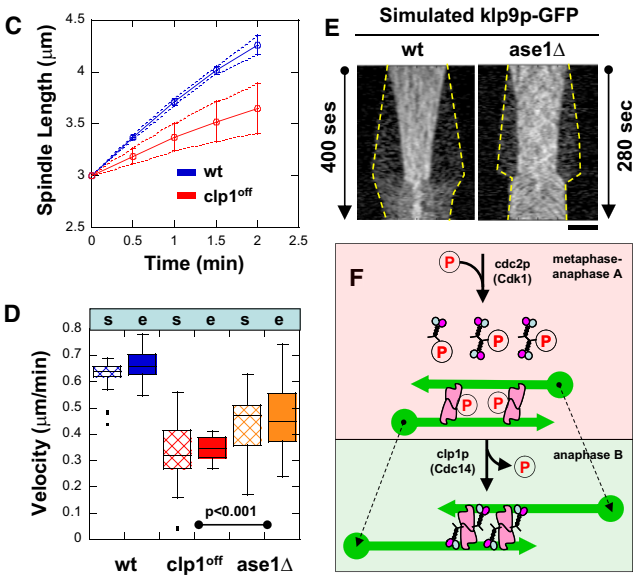

Figure 7. Cytosim Model of How Klp9p Motor and Ase1p MAP Interact for Proper Anaphase B

(A) Cytosim model assumption: klp9p is either parallel or antiparallel by itself, but is antiparallel when bound to ase1p. Bar, 1 μm.

(B) Parameters used in simulations (see text). Parameters of klp9p are assumed to be similar to Eg5, a similar mitotic kinesin.

(C) Comparative plot of spindle length versus time and box plot of anaphase B spindle elongation velocity of simulated wild-type cells (WT, blue) and mutant *clp1*^{off} cells (*clp1*^{off}, red). Simulation reproduces the experimental results (compare with Figure 4C).

(D) Comparative box plot of simulated (s) and experimental (e) spindle velocities for wild-type cells (WT, blue), *clp1*^{off} cells (*clp1*^{off}, red), and *ase1Δ* cells (*ase1Δ*, orange). Spindle velocities of *ase1Δ* cells are intermediate between WT and *clp1*^{off}.

(E) Comparative kymographs of simulated klp9p-GFP focusing at the middle of the spindle in wild-type and *ase1Δ* cells. Dashed yellow lines show positions of the spindle poles. In the absence of ase1p, klp9p is less focused at the spindle midzone, similar to experimental findings (compare with Figures 3B and 5C). Bar, 1 μm.

(F) Model of how kinase cdc2p (Cdk1) and phosphatase clp1p (Cdc14) regulate the function of klp9p (motor) and ase1p (MAP) for proper anaphase B.

DISCUSSION

Our current work examined all individual motors that may be involved in anaphase B spindle elongation in fission yeast and found that the kinesin-6 klp9p plays a major role (Figure 1E). We suggest a mechanism whereby a cdc2p and clp1p phosphorylation switch controls the interactions of klp9p and ase1p at the spindle midzone to initiate anaphase B spindle elongation (Figure 7F). Key to this mechanism may be the physical binding of the tetrameric kinesin-6 motor klp9p to the microtubule antiparallel bundling MAP ase1p. Imaging and FRAP analyses supported the conclusion of an in vivo interaction (Figure 6), and IP analyses confirmed an in vitro interaction between klp9p and ase1p (Figure 5A). Klp9p-ase1p binding in turn biases the orientation of the motor from being naturally flexible (Kapitein et al., 2005) to the more rigid and antiparallel configuration of the MAP (Janson et al., 2007). This conformational change may increase motor efficiency in microtubule sliding, as shown by computer simulations (Figure 7). The motor-MAP conformational change is an attractive model and will require future single-molecule or structural analyses to confirm.

Which other motors may contribute to microtubule sliding during anaphase B? Klp9p produces ~50% of the anaphase B velocity (Figures 1E and 2D). In the absence of klp9p, there is a residual ~0.3 μm/min spindle elongation velocity at room temperature (Figures 1E and 2D). Fission yeast has a second mitotic kinesin, kinesin-5 cut7p, which has been reported to localize to the spindle midzone and whose temperature-sensitive mutation caused monopolar spindles (Hagan and Yanagida, 1990, 1992). This suggests that cut7p acts at an earlier stage of mitosis to organize the bipolar spindle. Our studies extend these previous works by looking for possible roles of cut7p at anaphase B by using the *cut7-24* temperature-sensitive mutant and a temperature control device. We showed that the *cut7-24* mutant did not decrease anaphase B spindle elongation velocity (Figures 1C and 1E). Consistent with this finding, cut7p-3GFP does not localize to the spindle midzone during anaphase B (Figure 1D). Lack of localization of cut7p-3GFP at the spindle midzone in this study appears different than localization of immunofluorescent staining of cut7p to the spindle midzone in mitosis (but not the spindle midzone in meiosis) (Hagan and Yanagida, 1990, 1992). One explanation may be that anti-cut7p antibodies used for immunofluorescence may crossreact with other motors. We favor the explanation that cut7p may act in a redundant and back-up manner with klp9p to ensure anaphase B spindle elongation. Indeed, whereas we did not observe cut7p-3GFP at the spindle midzone in wild-type cells (Figure 1D), our preliminary result shows that cut7p-3GFP does localize to the spindle midzone in *klp9Δ* mutant cells, suggesting possible redundant roles (our unpublished data). In budding yeast, both kinesins and dynein play cooperative roles in bringing about proper anaphase spindle elongation (Saunders et al., 1995). Our current study deals with individual motors and showed that dynein deletion alone has no effect on spindle elongation (Figure 1E). Future studies will explore combinatorial relationships among the different motors for a fuller understanding of anaphase B.

Anaphase B is a prominent phase of mitosis, marked by an increase in spindle length, up to 1.5–4 times of the initial metaphase/anaphase A spindle length in different organisms (Hayashi et al., 2007). To date, physical mechanisms producing anaphase B have primarily focused on the kinesin-5 motors (Scholey et al., 2003; Sharp et al., 2000). Kinesin-6 motors have been assigned regulatory roles at the end of mitosis at the transition to cytokinesis (Gruneberg et al., 2006; Kuriyama et al., 2002; Matuliene

and Kuriyama, 2002; Mishima et al., 2002). Indeed, the centralspindlin complex, which contains kinesin-6, is regulated by aurora B kinase for proper cytokinesis (Mishima and Glotzer, 2003; Mishima et al., 2002, 2004). To our knowledge, the involvement of fission yeast klp9p in anaphase B spindle elongation suggests a novel function for the kinesin-6 family of motors. Our simulations, while not meant to represent actual klp9p kinetics, were useful in predicting and recapitulating our experimental results by showing trends in elongation velocities and how these rates can be altered by specific configurations of klp9p (Figure 7). Other models are also plausible. For example, klp9p-ase1p interaction can serve to concentrate klp9p at the spindle midzone, and cooperative effects of motors can lead to more efficient velocity. Alternatively, ase1p may act as a spacer between two microtubules to allow klp9p to enter and function, or ase1p may act as a brake to slow down klp9p movement. Future studies will need to examine the evolution of the multiple functions associated with the kinesin-6 family of mitotic motors.

The MAP Ase1/PRC1 appears to be a major scaffolding protein at the spindle midzone. The fission yeast ase1p is a substrate for cdc2p and clp1p phosphoregulation, which allows for binding to klp9p (this study). The budding yeast Ase1, and human PRC1, may also be a substrate for Cdk1 and Cdc14, and other regulatory proteins such as the Ipl1/aurora-B kinase (Jiang et al., 1998; Khmelinskii et al., 2007; Kotwaliwale et al., 2007). Our studies add to the emerging concept that the spindle midzone, with motors and MAPs and kinases and phosphatases, is a crowded mechanical and chemical machine (Glotzer, 2005).

EXPERIMENTAL PROCEDURES

Experimental procedures are described in the Supplemental Data.

SUPPLEMENTAL DATA

Supplemental Data include one figure, five tables, and Supplemental Experimental Procedures and can be found with this article online at http://www.cell.com/developmental-cell/supplemental/S1534-5807(09)00253-6/.

ACKNOWLEDGMENTS

We thank Anabelle Decottignies, Fred Chang, Kathy Gould, Ian Hagan, Dan McCollum, and Paul Nurse for yeast strains and reagents. We thank Andrea Stout for expert technical FRAP assistance. We also thank members of Erfei Bi Lab and members of MBL Physiology 2007 for helpful discussions and advice. F.J.N. is supported by BioMS, J.W. is supported by Volkswagen-Stiftung. G.V.-C. is supported by ARC. The Tran Lab is supported by grants from NIH, ACS, HFSP, ANR, FRM, and LaLigue. C.F., I.L., G. V.-C., and P.T.T. created the reagents, performed the experiments, and analyzed the data. J.W. and F.N. performed the computer simulations. C.F., J.W., F.N., and P.T.T. wrote the paper, and all authors made comments.

Received: February 14, 2009
Revised: May 8, 2009
Accepted: June 19, 2009
Published: August 17, 2009

REFERENCES

Brazer, S.C., Williams, H.P., Chappell, T.G., and Cande, W.Z. (2000). A fission yeast kinesin affects Golgi membrane recycling. Yeast *16*, 149–166.

Browning, H., Hayles, J., Mata, J., Aveline, L., Nurse, P., and McIntosh, J.R. (2000). Tea2p is a kinesin-like protein required to generate polarized growth in fission yeast. J. Cell Biol. *151*, 15–28.

Carminati, J.L., and Stearns, T. (1997). Microtubules orient the mitotic spindle in yeast through dynein-dependent interactions with the cell cortex. J. Cell Biol. *138*, 629–641.

Cheeseman, I.M., and Desai, A. (2008). Molecular architecture of the kinetochore-microtubule interface. Nat. Rev. Mol. Cell Biol. *9*, 33–46.

Cueille, N., Salimova, E., Esteban, V., Blanco, M., Moreno, S., Bueno, A., and Simanis, V. (2001). *Flp1*, a fission yeast orthologue of the *S. cerevisiae CDC14* gene, is not required for cyclin degradation or rum1p stabilisation at the end of mitosis. J. Cell Sci. *114*, 2649–2664.

Fink, G., Schuchardt, I., Colombelli, J., Stelzer, E., and Steinberg, G. (2006). Dynein-mediated pulling forces drive rapid mitotic spindle elongation in Ustilago maydis. EMBO J. *25*, 4897–4908.

Garcia, M.A., Koonrugsa, N., and Toda, T. (2002a). Spindle-kinetochore attachment requires the combined action of Kin I-like Klp5/6 and Alp14/Dis1-MAPs in fission yeast. EMBO J. *21*, 6015–6024.

Garcia, M.A., Koonrugsa, N., and Toda, T. (2002b). Two kinesin-like Kin I family proteins in fission yeast regulate the establishment of metaphase and the onset of anaphase A. Curr. Biol. *12*, 610–621.

Glotzer, M. (2005). The molecular requirements for cytokinesis. Science *307*, 1735–1739.

Gruneberg, U., Neef, R., Li, X., Chan, E.H., Chalamalasetty, R.B., Nigg, E.A., and Barr, F.A. (2006). KIF14 and citron kinase act together to promote efficient cytokinesis. J. Cell Biol. *172*, 363–372.

Guse, A., Mishima, M., and Glotzer, M. (2005). Phosphorylation of ZEN-4/MKLP1 by aurora B regulates completion of cytokinesis. Curr. Biol. *15*, 778–786.

Hagan, I.M. (1998). The fission yeast microtubule cytoskeleton. J. Cell Sci. *111*, 1603–1612.

Hagan, I., and Yanagida, M. (1990). Novel potential mitotic motor protein encoded by the fission yeast cut7+ gene. Nature *347*, 563–566.

Hagan, I., and Yanagida, M. (1992). Kinesin-related cut7 protein associates with mitotic and meiotic spindles in fission yeast. Nature *356*, 74–76.

Hayashi, T., Sano, T., Kutsuna, N., Kumagai-Sano, F., and Hasezawa, S. (2007). Contribution of anaphase B to chromosome separation in higher plant cells estimated by image processing. Plant Cell Physiol. *48*, 1509–1513.

Hiraoka, Y., Ding, D.Q., Yamamoto, A., Tsutsumi, C., and Chikashige, Y. (2000). Characterization of fission yeast meiotic mutants based on live observation of meiotic prophase nuclear movement. Chromosoma *109*, 103–109.

Hoyt, M.A., He, L., Loo, K.K., and Saunders, W.S. (1992). Two Saccharomyces cerevisiae kinesin-related gene products required for mitotic spindle assembly. J. Cell Biol. *118*, 109–120.

Janson, M.E., Loughlin, R., Loiodice, I., Fu, C., Brunner, D., Nedelec, F.J., and Tran, P.T. (2007). Crosslinkers and motors organize dynamic microtubules to form stable bipolar arrays in fission yeast. Cell *128*, 357–368.

Jiang, W., Jimenez, G., Wells, N.J., Hope, T.J., Wahl, G.M., Hunter, T., and Fukunaga, R. (1998). PRC1: a human mitotic spindle-associated CDK substrate protein required for cytokinesis. Mol. Cell *2*, 877–885.

Kapitein, L.C., Peterman, E.J., Kwok, B.H., Kim, J.H., Kapoor, T.M., and Schmidt, C.F. (2005). The bipolar mitotic kinesin Eg5 moves on both microtubules that it crosslinks. Nature *435*, 114–118.

Kapitein, L.C., Janson, M.E., van den Wildenberg, S.M., Hoogenraad, C.C., Schmidt, C.F., and Peterman, E.J. (2008a). Microtubule-driven multimerization recruits ase1p onto overlapping microtubules. Curr. Biol. *18*, 1713–1717.

Kapitein, L.C., Kwok, B.H., Weinger, J.S., Schmidt, C.F., Kapoor, T.M., and Peterman, E.J. (2008b). Microtubule cross-linking triggers the directional motility of kinesin-5. J. Cell Biol. *182*, 421–428.

Kapoor, T.M., Mayer, T.U., Coughlin, M.L., and Mitchison, T.J. (2000). Probing spindle assembly mechanisms with monastrol, a small molecule inhibitor of the mitotic kinesin, Eg5. J. Cell Biol. *150*, 975–988.

Khmelinskii, A., Lawrence, C., Roostalu, J., and Schiebel, E. (2007). Cdc14-regulated midzone assembly controls anaphase B. J. Cell Biol. *177*, 981–993.

Khodjakov, A., La Terra, S., and Chang, F. (2004). Laser microsurgery in fission yeast; role of the mitotic spindle midzone in anaphase B. Curr. Biol. *14*, 1330–1340.

Kotwaliwale, C.V., Frei, S.B., Stern, B.M., and Biggins, S. (2007). A pathway containing the Ipl1/aurora protein kinase and the spindle midzone protein Ase1 regulates yeast spindle assembly. Dev. Cell *13*, 433–445.

Kurasawa, Y., Earnshaw, W.C., Mochizuki, Y., Dohmae, N., and Todokoro, K. (2004). Essential roles of KIF4 and its binding partner PRC1 in organized central spindle midzone formation. EMBO J. *23*, 3237–3248.

Kuriyama, R., Gustus, C., Terada, Y., Uetake, Y., and Matuliene, J. (2002). CHO1, a mammalian kinesin-like protein, interacts with F-actin and is involved in the terminal phase of cytokinesis. J. Cell Biol. *156*, 783–790.

Kwok, B.H., Kapitein, L.C., Kim, J.H., Peterman, E.J., Schmidt, C.F., and Kapoor, T.M. (2006). Allosteric inhibition of kinesin-5 modulates its processive directional motility. Nat. Chem. Biol. *2*, 480–485.

Loiodice, I., Staub, J., Setty, T.G., Nguyen, N.P., Paoletti, A., and Tran, P.T. (2005). Ase1p organizes antiparallel microtubule arrays during interphase and mitosis in fission yeast. Mol. Biol. Cell *16*, 1756–1768.

Maiato, H., Sampaio, P., and Sunkel, C.E. (2004). Microtubule-associated proteins and their essential roles during mitosis. Int. Rev. Cytol. *241*, 53–153.

Mallavarapu, A., Sawin, K., and Mitchison, T. (1999). A switch in microtubule dynamics at the onset of anaphase B in the mitotic spindle of Schizosaccharomyces pombe. Curr. Biol. *9*, 1423–1426.

Matuliene, J., and Kuriyama, R. (2002). Kinesin-like protein CHO1 is required for the formation of midbody matrix and the completion of cytokinesis in mammalian cells. Mol. Biol. Cell *13*, 1832–1845.

Mishima, M., and Glotzer, M. (2003). Cytokinesis: a logical GAP. Curr. Biol. *13*, R589–R591.

Mishima, M., Kaitna, S., and Glotzer, M. (2002). Central spindle assembly and cytokinesis require a kinesin-like protein/RhoGAP complex with microtubule bundling activity. Dev. Cell *2*, 41–54.

Mishima, M., Pavicic, V., Gruneberg, U., Nigg, E.A., and Glotzer, M. (2004). Cell cycle regulation of central spindle assembly. Nature *430*, 908–913.

Mogilner, A., Wollman, R., Civelekoglu-Scholey, G., and Scholey, J. (2006). Modeling mitosis. Trends Cell Biol. *16*, 88–96.

Mollinari, C., Kleman, J.P., Jiang, W., Schoehn, G., Hunter, T., and Margolis, R.L. (2002). PRC1 is a microtubule binding and bundling protein essential to maintain the mitotic spindle midzone. J. Cell Biol. *157*, 1175–1186.

Nabeshima, K., Nakagawa, T., Straight, A.F., Murray, A., Chikashige, Y., Yamashita, Y.M., Hiraoka, Y., and Yanagida, M. (1998). Dynamics of centromeres during metaphase-anaphase transition in fission yeast: Dis1 is implicated in force balance in metaphase bipolar spindle. Mol. Biol. Cell *9*, 3211–3225.

Nedelec, F.J., and Foethke, D. (2007). Collective Langevin dynamics of flexible cytoskeletal fibers. N. J. Phys. *9*, 427.

Nguyen-Ngoc, T., Afshar, K., and Gonczy, P. (2007). Coupling of cortical dynein and G alpha proteins mediates spindle positioning in Caenorhabditis elegans. Nat. Cell Biol. *9*, 1294–1302.

O'Connell, C.B., and Wang, Y.L. (2000). Mammalian spindle orientation and position respond to changes in cell shape in a dynein-dependent fashion. Mol. Biol. Cell *11*, 1765–1774.

Pidoux, A.L., LeDizet, M., and Cande, W.Z. (1996). Fission yeast pkl1 is a kinesin-related protein involved in mitotic spindle function. Mol. Biol. Cell *7*, 1639–1655.

Roof, D.M., Meluh, P.B., and Rose, M.D. (1992). Kinesin-related proteins required for assembly of the mitotic spindle. J. Cell Biol. *118*, 95–108.

Sagolla, M.J., Uzawa, S., and Cande, W.Z. (2003). Individual microtubule dynamics contribute to the function of mitotic and cytoplasmic arrays in fission yeast. J. Cell Sci. *116*, 4891–4903.

Saunders, W.S., Koshland, D., Eshel, D., Gibbons, I.R., and Hoyt, M.A. (1995). Saccharomyces cerevisiae kinesin- and dynein-related proteins required for anaphase chromosome segregation. J. Cell Biol. *128*, 617–624.

Schmidt, D.J., Rose, D.J., Saxton, W.M., and Strome, S. (2005). Functional analysis of cytoplasmic dynein heavy chain in Caenorhabditis elegans with fast-acting temperature-sensitive mutations. Mol. Biol. Cell *16*, 1200–1212.

Scholey, J.M., Brust-Mascher, I., and Mogilner, A. (2003). Cell division. Nature *422*, 746–752.

Schuyler, S.C., Liu, J.Y., and Pellman, D. (2003). The molecular function of Ase1p: evidence for a MAP-dependent midzone-specific spindle matrix. Microtubule-associated proteins. J. Cell Biol. *160*, 517–528.

Sharp, D.J., Rogers, G.C., and Scholey, J.M. (2000). Microtubule motors in mitosis. Nature *407*, 41–47.

Straight, A.F., Sedat, J.W., and Murray, A.W. (1998). Time-lapse microscopy reveals unique roles for kinesins during anaphase in budding yeast. J. Cell Biol. *143*, 687–694.

Tanaka, T.U., and Desai, A. (2008). Kinetochore-microtubule interactions: the means to the end. Curr. Opin. Cell Biol. *20*, 53–63.

Tolic-Norrelykke, I.M., Sacconi, L., Thon, G., and Pavone, F.S. (2004). Positioning and elongation of the fission yeast spindle by microtubule-based pushing. Curr. Biol. *14*, 1181–1186.

Trautmann, S., Wolfe, B.A., Jorgensen, P., Tyers, M., Gould, K.L., and McCollum, D. (2001). Fission yeast Clp1p phosphatase regulates G2/M transition and coordination of cytokinesis with cell cycle progression. Curr. Biol. *11*, 931–940.

Trautmann, S., Rajagopalan, S., and McCollum, D. (2004). The *S. pombe* Cdc14-like phosphatase Clp1p regulates chromosome biorientation and interacts with Aurora kinase. Dev. Cell *7*, 755–762.

Troxell, C.L., Sweezy, M.A., West, R.R., Reed, K.D., Carson, B.D., Pidoux, A.L., Cande, W.Z., and McIntosh, J.R. (2001). pkl1(+)and klp2(+): Two kinesins of the Kar3 subfamily in fission yeast perform different functions in both mitosis and meiosis. Mol. Biol. Cell *12*, 3476–3488.

Valentine, M.T., Fordyce, P.M., and Block, S.M. (2006a). Eg5 steps it up! Cell Div. *1*, 31.

Valentine, M.T., Fordyce, P.M., Krzysiak, T.C., Gilbert, S.P., and Block, S.M. (2006b). Individual dimers of the mitotic kinesin motor Eg5 step processively and support substantial loads in vitro. Nat. Cell Biol. *8*, 470–476.

Verni, F., Somma, M.P., Gunsalus, K.C., Bonaccorsi, S., Belloni, G., Goldberg, M.L., and Gatti, M. (2004). Feo, the Drosophila homolog of PRC1, is required for central-spindle formation and cytokinesis. Curr. Biol. *14*, 1569–1575.

West, R.R., Malmstrom, T., Troxell, C.L., and McIntosh, J.R. (2001). Two related kinesins, klp5+ and klp6+, foster microtubule disassembly and are required for meiosis in fission yeast. Mol. Biol. Cell *12*, 3919–3932.

West, R.R., Malmstrom, T., and McIntosh, J.R. (2002). Kinesins klp5(+) and klp6(+) are required for normal chromosome movement in mitosis. J. Cell Sci. *115*, 931–940.

Wilson-Grady, J.T., Villen, J., and Gygi, S.P. (2008). Phosphoproteome analysis of fission yeast. J. Proteome Res. *7*, 1088–1097.

Wolfe, B.A., McDonald, W.H., Yates, J.R., 3rd, and Gould, K.L. (2006). Phospho-regulation of the Cdc14/Clp1 phosphatase delays late mitotic events in S. pombe. Dev. Cell *11*, 423–430.

Yamashita, A., Sato, M., Fujita, A., Yamamoto, M., and Toda, T. (2005). The roles of fission yeast ase1 in mitotic cell division, meiotic nuclear oscillation, and cytokinesis checkpoint signaling. Mol. Biol. Cell *16*, 1378–1395.

Zhu, C., and Jiang, W. (2005). Cell cycle-dependent translocation of PRC1 on the spindle by Kif4 is essential for midzone formation and cytokinesis. Proc. Natl. Acad. Sci. USA *102*, 343–348.

Zhu, C., Bossy-Wetzel, E., and Jiang, W. (2005). Recruitment of MKLP1 to the spindle midzone/midbody by INCENP is essential for midbody formation and completion of cytokinesis in human cells. Biochem. J. *389*, 373–381.

Zhu, C., Lau, E., Schwarzenbacher, R., Bossy-Wetzel, E., and Jiang, W. (2006). Spatiotemporal control of spindle midzone formation by PRC1 in human cells. Proc. Natl. Acad. Sci. USA *103*, 6196–6201.